scientific reports

Check for updates

OPEN

On solution existence of MHD Casson nanofluid transportation across an extending cylinder through porous media and evaluation of priori bounds

Sohaib Abdal[1], Sajjad Hussain[2], Imran Siddique[3], Ali Ahmadian[4,5]✉ & Massimiliano Ferrara[5]

It is a theoretical exportation for mass transpiration and thermal transportation of Casson nanofluid over an extending cylindrical surface. The Stagnation point flow through porous matrix is influenced by magnetic field of uniform strength. Appropriate similarity functions are availed to yield the transmuted system of leading differential equations. Existence for the solution of momentum equation is proved for various values of Casson parameter β, magnetic parameter M, porosity parameter K_p and Reynolds number Re in two situations of mass transpiration (suction/injuction). The core interest for this study aroused to address some analytical aspects. Therefore, existence of solution is proved and uniqueness of this results is discussed with evaluation of bounds for existence of solution. Results for skin friction factor are established to attain accuracy for large injection values. Thermal and concentration profiles are delineated numerically by applying Runge-Kutta method and shooting technique. The flow speed retards against M, β and K_p for both situations of mass injection and suction. The thermal boundary layer improves with Brownian and thermopherotic diffusions.

Nomenclature

u	Radial velocity component
w	Axial velocity component
a	Radius of cylinder
c	Strain rate of oncoming radial flow
Nb	Brownian motion
D_B	Brownian diffusion coefficient
Le	Lewis number
T	Non-dimensional temperature
C	Non-dimensional nanoparticles concentration
C_w	Nanoparticles concentration at surface
C_∞	Nanoparticles concentration away from the surface
Nu_x	Nusselt number
Pr	Prandtl number
C_{fx}	skin friction
Sh_x	Sherwood number
Nt	Thermophoresis parameter
D_T	Thermophoretic diffusion coefficient
T_w	Temperature at surface

[1]School of Mathematics, Northwest University, No.229 North Taibai Avenue, Xi'an 7100069, China. [2]School of Aerospace and Mechanical Engineering, Nanyang Technological University, Singapore, Singapore. [3]Department of Mathematics, University of Management and Technology, Lahore, Pakistan. [4]Institute of IR 4.0, The National University of Malaysia, UKM, 43400, Bangi, Selangor, Malaysia. [5]Department of Law, Economics and Human Sciences & Decisions Lab, University Mediterranea of Reggio Calabria, Reggio Calabria, Italy. ✉email: ahmadian.hosseini@gmail.com

T_∞ Temperature away from the surface
Re Reynolds number
M Magnetic field
K_p Permeability of porous medium
U_w Velocity of stretching sheet.

Greek symbols
ρ Density of fluid
ν Kinematic viscosity
τ Ratio between hear capacities of the fluid and nanoparticles
μ Dynamic viscosity
γ Permeability parameter
α Thermal diffusivity
θ Dimensionless temperature
ν Kinematic viscosity
β Casson parameter
Φ Nanoparticles volume fraction.

Non Newtonian fluids do not satisfy the Newton's law of viscosity e.g. juice of apple, fuel oils, cream, honey, blood, toothpaste etc. Casson fluid is a prominent type of fluid among all of them. It is claimed that for some fluids this rheological model is better as compared to the viscoelastic model. This model is suitable for blood as well as for chocolate rheology. Basically, the sample of casson fluids is made up due to the connections or interactions between the phases of liquids and solid. When yield stress becomes compulsory and it is lower than the shear stress, Cason fluids behaves like solids. e.g. Soup, tomato, honey, etc. Human blood is also an example of Casson fluid. Shah et al.[1] investigated the flow of Casson nano fluid along with activation energy as well as the chemical reaction by using the stretched surface. Oyelakin et al.[2] studied gyrotactic micro-organism in Casson nano-fluid flow. Reza et al.[3] utilized finite difference analysis on unsteady MHD flow of Casson fluid. Effect of slip boundary conditions of time dependent Casson nano-fluid passing over sheet were discussed by Oyelakin et al.[4,5]. Mondal et al.[6] discussed three dimensional casson nano-fluid over a porous stretch sheet. Non-Newtonian fluid together with various geometries are studied in[7–10].

Some analytical uses of straight-line flows along with the stretching/shrinking sheet or by the regular string consist in different processing of collecting i.e. industry of polymer, a porous stretching/shrinking of plastic films, artificial filaments, fibers of counterfeit, melting of metals, expulsion of metals, persistent throwing, glass blowing etc.[11]. Firstly, the problem of the stretching sheet was discussed by Sakiadis[12,13]. Awaludin et.al.[14] discussed the boundary layer flow of magnetohydrodynamic over stretching and shrinking sheet. Dzulkifli et. al.[15] analyzed the flow of stagnation point as well as relocation of heat over stretching and stretching sheet by using the nano fluid along with the impact of slip velocity. Bakar et.al.[16] disussed on analysis of relocation of heat along with the nanofluid by using stretching / shrinking surface with the impact of suction. Malvandi et al.[17] discussed about the flow of stagnation point by using the nonlinear stretching/shrinking sheet which is a porous surface.

In 1942, Haanas Alfren introduced terminology of MHD "Magnetohydrodynamic". Large number scholars has done researches to understand the properties of MHD and to check these properties impact with various terms of nanofluid Now a days using in various fields of life such as astrophysics, medical science, geography, and many other. Impact of activation energy of Arrhenius over a nonlinear stretching surface with convective third grade nanofluid in MHD flow investigated by Hayat et al.[18]. Nanomaterials treatment regardless of the imposition of MHD streamline considering the melting sheet reviewed by Dinh et al.[19]. Explored MHD nanofluid flow over a porous formation of shrinking walls of entropy conducted by Rashid et al.[20]. Research taken on magnetohydrodynamic current of nanofluid through a vertical permeable plate that flows semi-infinitely by Pavar et al.[21]. Oyelakin et al.[22] discussed MHD flow of tangent hyperbolic. Chen et al.[23] studied Mixed convection nanofluid stream in vertical channel entropy production in magnetohydrodynamic. Arifuzzaman et al.[24] studied heat and mass transfer analysis of MHD through a porous plate.

Nano liquids are potential heat exchange fluids with improved thermos-physical properties and heat trade execution can be associated with various tools for better exhibitions Work nowadays in the area of nano-materials grown rapidly due to its comprehensive implementations in variety of fields. Scholars paid so interest in recent array in this field due to their various applications, heat and mass transfer[25], in the engineering and industrial appliances sector, for example Nuclear reactor cooling, furnace, coolant, polymer Process, filament plastics. Improving fluid thermal conductivity of nanoparticles studied by Choi and Eastman[26]. Nanofluid jet cooling fluid flow and heat transfer analysis on a hot surface with varying roughness studded by Mahdavi et al.[27]. Oyelakin et al.[28] discussed non-linear radiation in Casson nano-fluid flow. Bagh et al.[29] discussed time dependent water based nano fluid on an extending sheet. Ali et al.[30] studied the impact of Stefan blowing for nanofluid flow. Three dimensional casson-carreau nanofluid flow numerical scrutinization interrogated by Shahid et al.[31]. Reza et al.[32] studied multiphase behavior of fluid flow with nanoparticles. Sadeghi et al.[33] studied ferro-fluid with the presence of two cylinders. Seyyedi et al.[34] solved different shape nano-particles by using entropy generation. Dogonchi et al.[35] investigated heat and mass transfer effects of nanofluid in an irregular triangular enclosure. Similar work were done by[36–40].

A glance of the related studies of flow across a cylindrical surface is mostly treated with implementation of numerical methods. Mastroberardino and Siddique[41] presented numerical solution for MHD flow of Newtonian fluid towards a stretching cylinder. They discussed the conditions for existence and uniqueness of the solution. Motivated from this rarely considered work we studied the fluid flow through porous medium in the existence of applied magnetic field. To our interest we proved the existence and uniqueness of this extended fluid flow

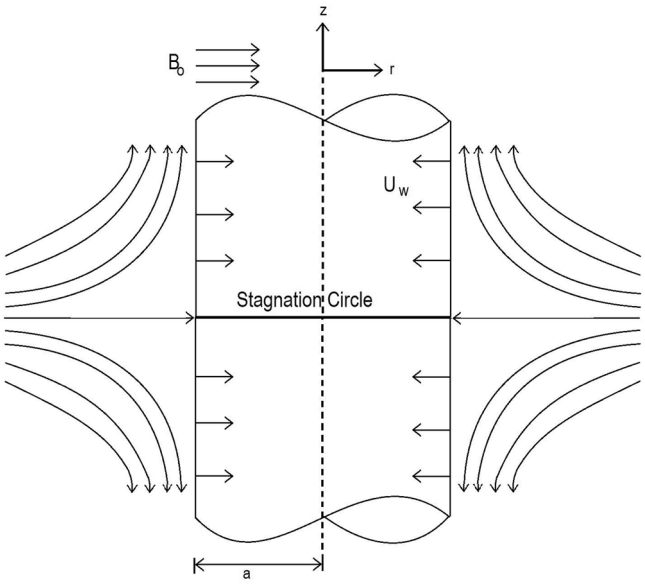

Figure 1. Physical configuration and coordinate system.

problem. we also evaluated the priori bounds for skin friction factor, As for as we know these aspects for the flow of Casson fluids are never explained in the existing studies. The innovation of the work highlighted the existence of solution with uniqueness of results and bounds for skin friction. Moreover, numerical solution of this work is obtained by employing shooting base numerical method codded in matlab script. This exploration may find application in blood rheology, food processing and metallurgy.

Mathematical analysis

In this segment, we are concerned with the following incompressible Casson nanofluid model[42]

$$\left.\begin{aligned} \partial_t \rho + u.\nabla\rho = 0 \\ \rho(\partial_t u + u.\nabla u) = -\nabla\rho - (1+\frac{1}{\beta})\mu\Delta u - f \\ div\ u = 0 \\ \partial_t T + div(u\ T) = \frac{k}{\rho C_p}\nabla^2 T + \tau(D_B\ \partial_r T\ \partial_r C + \frac{D_T}{T_\infty}(\partial_r T)^2) \\ \partial_t C + div(u\ C) = D_B\ \nabla^2 C + + \frac{D_T}{T_\infty}(\partial_r T)^2 \end{aligned}\right\} \tag{1}$$

Consider an incompressible and electrically conducting Casson fluid which flows steady state across an axially extending cylinder of radius = a. Velocity of the stretching wall of the cylinder is $U_w = ca\gamma$. The mass suction across the wall is $w_w = 2cz$, Here c is strain rate of the radial flow and γ is permeability parameter. The fluid flows through a porous medium of Darcy resistance. There is a non varying magnetic field of intensity B_o that acts normally to the axis of symmetry (see Fig. 1). The temperature T_w and concentration C_w are taken at the cylinder and T_∞ and C_∞ are the far field temperature and concentration. Casson fluid parameter is β and k' is the porosity of medium. The formulation in (r, θ, z) is constituted keeping in view with the assumptions as mentioned above.

$$\left.\begin{aligned} \frac{\partial(rw)}{\partial z} + \frac{\partial(ru)}{\partial r} = 0, \\ w\frac{\partial w}{\partial z} + u\frac{\partial w}{\partial r} = \nu(1+\frac{1}{\beta})(\frac{\partial^2 w}{\partial r^2} + \frac{1}{r}\frac{\partial w}{\partial r}) - \frac{\sigma B_0^2 w}{\rho} - \frac{\nu}{k'}w, \\ w\frac{\partial T}{\partial z} + u\frac{\partial T}{\partial r} = \alpha(\frac{\partial^2 T}{\partial r^2} + \frac{1}{r}\frac{\partial T}{\partial r}) + \tau(D_B\frac{\partial T}{\partial r}\frac{\partial C}{\partial r} + (\frac{\partial T}{\partial y})^2\frac{D_T}{T_\infty}), \\ w\frac{\partial C}{\partial z} + u\frac{\partial C}{\partial y} = D_B(\frac{\partial^2 C}{\partial r^2} + \frac{1}{r}\frac{\partial C}{\partial r}) + \frac{D_T}{T_\infty}\frac{1}{r}(\frac{\partial}{\partial r}(r\frac{\partial T}{\partial r})). \end{aligned}\right\} \tag{2}$$

with boundary conditions:

$$\left.\begin{aligned} u = U_w,\ w = w_w,\ T = T_w,\ C = C_w,\ at\ r = a, \\ w \to 0,\ T \to T_\infty,\ C \to C_\infty,\ as\ r \to \infty. \end{aligned}\right\} \tag{3}$$

In order to yield dimensionless form, similarity transformations are entitled as:

$$\xi = (\frac{r}{a})^2,\ u = -ca\frac{f(\xi)}{\sqrt{\xi}},\ w = 2cf'(\xi)z,\ \theta(\xi) - \frac{T - T_\infty}{T_w - T_\infty} = 0,\ \phi(\xi) - \frac{C - C_\infty}{C_w - C_\infty} = 0.\Big\} \tag{4}$$

The first expression in (2) becomes an identity and the remaining's take the form as follows:

$$(1 + \frac{1}{\beta})\xi f''' + f'' - Re[f'^2 - ff''] - (M + K_p)f' = 0 \tag{5}$$

$$\xi\theta'' + (1 + PrRef)\theta' + \xi Pr[Nb\theta'\phi' + Nt\theta'^2] = 0 \tag{6}$$

$$\xi\phi'' + (1 + LeRef)\phi' + \frac{Nt}{Nb}[\xi\theta'' + \theta'] = 0 \tag{7}$$

Where the expression (3) are transformed:

$$\left.\begin{aligned} f(1) = \gamma,\ f'(1) = 1,\ \theta(1) = 1,\ \phi(1) = 1, \\ f'(\infty) \to 0,\ \theta(\infty) \to 0,\ \phi(\infty) \to 0, \end{aligned}\right\} \tag{8}$$

Where $M = \frac{\sigma B_0^2 a^2}{4\nu\rho}$ is magnetic parameter, $Re = \frac{ca^2}{2\nu}$ is Reynolds number, $Pr = \frac{\nu}{\alpha}$ is Prandtl number, $Nb = \frac{\tau D_B(C_w - C_\infty)}{\nu}$ is Brownian motion, $Nt = \frac{\tau D_T(T_w - T_\infty)}{T_\infty \nu}$ is thermophoresis parameter, $Le = \frac{\nu}{D_B}$ represents Lewis number. The physical quantities of interest are Cf_x (skin friction coefficient), Nu_x (local Nusselt number) and Sh_x (local Sherwood number):

$Cf_x = \frac{\tau_w}{\rho U^2 w}, Nu_x = \frac{aq_w}{k(T_w - T_\infty)}, Sh_x = \frac{xq_m}{D_B(C_w - C_\infty)}$,

where τ_w, q_w and q_m denotes shear stress, surface heat flux and surface mass flux,

$\tau_w = \mu\frac{\partial w}{\partial r}, q_w = -K\frac{\partial T}{\partial r}, q_m = -D_B\frac{\partial C}{\partial r}$ at $r = a$,

On solving these quantities with the help of given similarity transformation, we obtain:

$C_f(Re_x)^{-1/2} = (f''(1), Nu_x(Re_x)^{-1/2} = -2\theta'(1), Sh_x(Re_x)^{-1/2} = -2\phi'(1)$,

where, $(Re_x) = \frac{xU_w}{\nu}$ is the local Reynolds number.

Existence

Consider the BVP (boundary value problem)

$$(1 + \frac{1}{\beta})\xi f''' + f'' - Re[f'^2 - ff''] - (M + K_p)f' = 0 \tag{9}$$

with

$$f(1) = \gamma,\ f'(1) = 1, f'(\infty) \to 0.$$

In order to get the corresponding IVP (initial value problem), the missing initial condition is assumed to be

$$f''(1) = \epsilon, \tag{10}$$

Here ϵ, is a free parameter is relevant to skin friction parameter and $f(\xi;\epsilon)$ denotes the solution. It is because an IVP can be uniquely solved (locally). Thus, a topological shooting argument for some choice of ϵ. For convince, the dependence of f on ϵ may be skipped for some time. The existence of $f'(\xi;\epsilon)$ for all $\xi > 1$ to satisfy Eq. (8). It may yield a solution to BVP. Two sets X and Y are taken as:

$$X = \epsilon < 0 |\ a\ first\ point\ \xi_X > 1\ is\ such\ that\ f'(\xi) > 0\ and\ f''(\xi_X) = 0\ on\ [1, \xi_X]$$

and

$$Y = \epsilon < 0 |\ a\ first\ point\ \xi_Y > 1\ such\ that\ f'(\xi) < 0\ and\ f''(\xi_Y) = 0\ on\ [1, \xi_Y]$$

Both of these sets are shown to be open and non-empty in the two Lemmas below:

Lemma 1 *The set X is non-empty and open.*

Proof From Eqs. (9) and (10), for $\xi = 1$,

$$(1+\frac{1}{\beta})f'''(1) = Re - \epsilon[(1+\frac{1}{\beta}) + R\gamma] + (M+k_p) \tag{11}$$

When $\epsilon = 0$, it implies that $f'''(1) = Re > 0$. Then initially $f' > 1$ and $f'' > 0$ on $(1, 1+\delta]$ for some $\delta > 0$. The continuity of the solutions of IVP and for $\epsilon < 0$ approaching zero, $f'(\xi;\epsilon)$ approaches $f'(\xi;0)$, i.e., $f'(\xi;\epsilon) > 0$ on $(1, 1+\delta]$ with $f(1+\delta;\epsilon) > 1$. But $f'(\xi;\epsilon) < 1$ and non-increasing for $\xi \in (1, 1+\delta_1)$ for some $0 < \delta_1 < \delta$. f' is to have a minimum if it is to go over 1. So the existence of first point ξ_X such that $f''(\xi_X;\epsilon) = 0$ and $f'(\xi_X;\epsilon) > 0$ on $[1, \xi_X]$. Therefore in case of $\epsilon < 0$ approaching to 0 this implies that ϵ belong to A. In order to show that X is open, let $\bar{\epsilon} \in X$ is open, let $\bar{\epsilon}X$. It is to show that all ϵ approaching $\bar{\epsilon}$ are in X. Then $f''(\xi_X) = 0$ and $0 < f'(\xi_X) < 1$. At $\xi_X(\bar{\epsilon})$, the Eq. (5) yields

$$f'''(\xi_X) = \frac{1}{(1+\frac{1}{\beta})\xi_X}[Ref'^2(\xi_X) + (M+K_p)f'(\xi_X)] > 0.$$

As the situation for IVP is continuous in its initial conditions, ϵ is approaching close to $\bar{\epsilon}$, $f''(\xi;\epsilon)$ has a root $\xi X(\epsilon)$, near $\xi X(\bar{\epsilon})$ with $f'(\xi;\epsilon) > 0$. Thus $\epsilon \in X$. We are there with the only possibility that $f'' = 0$ and $f' = 0$ simultaneously. When these values are substituted in Eq. (5), then $f''' = 0$ to imply $f'(\xi) = 0$ for all ξ. This is a contradiction to Eq. (8). □

Lemma 2 *The set Y is open and non-empty.*

Proof Equation (5) after integration yields as:

$$(1+\frac{1}{\beta})\xi f''(\xi) = (1+\frac{1}{\beta})\epsilon + Re\int_1^{\xi}(f'^2(z) - f(z)f''(z))dz + (M+K_p)(f(\xi)-\gamma) \tag{12}$$

and a subsequent integration by parts yields

$$(1+\frac{1}{\beta})\xi f''(\xi) = (1+\frac{1}{\beta})\epsilon + 2Re\int_1^{\xi} f'^2(z)dz + Re[\gamma - f(\xi)f'(\xi) + (M+K_p)(f(\xi)-\gamma)] \tag{13}$$

It is to show that there is $\epsilon < 0$, such that f' is equated to zero in the interval (1,2], say, before $f'' = 0$ in strict. Suppose this assertion is not true and consider.

Case (1A). Taking $f'' < 0$, $0 < f' < 1$ for $\xi \in (1,2]$, when $\gamma \geq 0$: By integrating $0 < f' < 1$ yields $\gamma < f < \gamma + \xi - 1$ on (1,2]. Then Eq. (13), provides:

$$f'' < [\frac{\epsilon}{2} + 2Re + Re\gamma + (M+k_p)](1+\frac{1}{\beta})$$

By selecting $\epsilon < -2(M+K_p) - 2Re\gamma - 4Re - 2$ to have $f'' < -1(1+\frac{1}{\beta})$ on (1,2] and thus $f'(2) < 0$ which contradicts $f' > 0$ on (1,2].

Case (1B). $f'' < 0$, $0 < f' < 1$ for $\xi \in (1,2]$, $\gamma < 0$. Also, the integration of $0 < f' < 1$ on (1,2] yields $\gamma < f < \gamma + \xi - 1$ on (1,2]. By employing these conditions in Eq. (13) to get

$$f'' < [\frac{\epsilon}{2} + 2Re + Re\gamma + (M+k_p)](1+\frac{1}{\beta})$$

Choosing $\epsilon < -2(M+K_p) - 4Re - 2$ then $f'' < -1(1+\frac{1}{\beta})$ on (1,2] and $f'(2) < 0$, it is a contradiction to $f' > 0$ on (1,2].

Case (2). If there is first point $\xi_1 \in (1,2]$ when $f''(\xi_1) = 0$ with $f'' < 0$ on $(1, \xi_1)$. By taking conditions on f'' as in case (1), it results in

$$\left.\begin{aligned} f'' < [2Re + \frac{\epsilon}{2}], when\gamma < 0, \\ f'' < [Re\gamma + 2Re + \frac{\epsilon}{2}], when\gamma \geq 0. \end{aligned}\right\}$$

for $\xi \in (1, \xi_1]$. Choosing

$$\left.\begin{aligned} f'' < [-4Re, when\gamma < 0, \\ f'' < -(2Re\gamma + 4Re), when\gamma \geq 0. \end{aligned}\right\}$$

implies that $f''(\xi_1) < 0$ it contradicts $f''(\xi_1) = 0$.

Case (3). We are left with options that $f'' = 0$ and $f' = 0$, but the process of Lemma 1, yields that $f' \equiv 0$ to contradict Eq. (8).

Hence Y is non void. Now it is to see that Y is open, let $\bar{\epsilon} \in Y$ with existence of $\xi_Y(\bar{\epsilon})$ such that $f''\xi_Y(\bar{\epsilon}) < 0$ and $f'\xi_Y(\bar{\epsilon}) = 0$. The continuity of the solution of IVP, for ϵ close to $\bar{\epsilon}$, there exist $\xi_Y(\epsilon)$ with $f''\xi_Y(\epsilon) < 0$ and $f'\xi_Y(\epsilon) = 0$, and so, Y is open.

Thus X and Y are non empty, disjoint and open sets, but $(-\infty, 0)$ is connected and so $XUY \neq (-\infty, 0)$. Thus, there is ϵ^* such that $\epsilon^* \notin X$ and $\epsilon^* \notin Y$. As already noticed it in not possible to have $f' = 0$ and $f'' = 0$ simultaneously; thus, thus only choice is $f''(\xi; \epsilon^*) < 0$ and $f'(\xi; \epsilon^*) > 0$ for all $\xi > 1$.

Since f' is bounded below and decreasing, $f'(\infty; \epsilon^*) = Z$ exists where $0 \leq Z < 1$. It is to see that $Z = 0$. We let $0 \leq Z < 1$. As $f'' < 0$ for $\xi > 1$, f' is bounded below by $Z > 0$, and so, f approaches to positive infinity. Finally the term ff'' is negative. Equation (5) provides as below:

$$\xi f'''(\xi) = \left[-f''(\xi) - (1 + \frac{1}{\beta})^{-1}\left[Re(ff'' - f'^2) + (M + K_p)f'(\xi)\right]\right] > ReC^2 = K > 0$$

for ξ to be large enough, there exists a point $\xi_2 > 1$ and $\xi > \xi_2$ to imply that

$$\xi f'''(\xi) > \frac{K}{2}$$

By integrating the above expression

$$f''(\xi) > f''(\xi_2) + \frac{K}{2}[ln\ \xi - ln\ \xi_2]\ for\ \xi > \xi_2,$$

Let $\xi \to \infty$ then $f'' \to \infty$, it contradicts to the fact that $f'' < 0$. Hence we have $f'(\infty; \epsilon^*) = 0$ the following theorem is established. □

Theorem 1 *There exists a solution to the boundary value problem for any* $Re > 0$ *and* $-\infty < \gamma < \infty$, *to satisfy* $f'(\xi) > 0$ *and* $f''(\xi) < 0$ *for all* $\xi > 1$.

Uniqueness

Now, we prove uniqueness of results:

Theorem 2 *If* $-\infty < \gamma < \infty$ *and* $Re > 0$, *then we cannot have two solutions for BVP (see 8)*

$$(1 + \frac{1}{\beta})\xi f''' + f'' - Re(f'^2 - ff'') - (M + K_p)f' = 0$$

when $f'(\xi) > 0$.

Proof From Eq. (5), $f'(\xi; \epsilon^*)$ cannot attain maximum. Thus for a solution with $f'(\xi; \epsilon^*) > 0$, $f''(\xi; \epsilon^*) < 0$. So for any positive solution $0 < f'(\xi; \epsilon^*) < 1$. Let $v = \frac{\partial f}{\partial \alpha}$. The differentiation of Eq. (5) with respect to ξ yields:

$$(1 + \frac{1}{\beta})\xi f^{iv} + f''' - Re[2f'f'' - ff''' - f'f''] - (M + K_p)f'' = 0 \tag{14}$$

$$(1 + \frac{1}{\beta})\xi v''' + v'' - Re[2f'v' - vf'' - fv''] - (M + K_p)v' = 0 \tag{15}$$

associated with

$$v(1) = v'(1) = 0, v''(1) = 1. \tag{16}$$

Thus for $\xi > 1$, we have v' positive and increasing and $v' > 0$ and increasing for $\xi > 1$.

It is to show a positive maximum does not exists for $v'(\xi, \epsilon^*)$. Let a maximum exists at first point for which $v > 0, v' > 0, v'' = 0$ and $v''' \leq 0$. Substituting $v'' = 0$ into Eq. (15) yields

$$(1 + \frac{1}{\beta})\xi v''' = Re[2f'v' - vf''] + (M + K_p)v' > 0 \tag{17}$$

It becomes contrary and hence v' cannot have a maxima. So $v' = \frac{\partial f'}{\partial \alpha} > 0$.

IF we let two solutions $f'(\xi; \epsilon^*)$ and $f'(\xi; \epsilon^{**})$ with $\epsilon^{**} > \epsilon^*$, and using Mean Value Theorem

$$f'(\xi; \epsilon^{**}) - f'(\xi; \epsilon^*) = (\frac{\partial f'}{\partial \epsilon})_{\epsilon = \hat{\epsilon}}(\epsilon^{**} - \epsilon^*) = v'(\xi; \hat{\epsilon})(\epsilon^{**} - \epsilon^*) \tag{18}$$

where $\epsilon^* < \hat{\epsilon} < \epsilon^{**}$. Now v' is bounded below by $L > 0$ for ξ large as it cannot have a maximum. Suppose $M = L(\epsilon^{**} - \epsilon^*)$ and $\xi \to \infty$, From Eq. (18), $0 = 1 - 1 = f'(\xi; \epsilon^{**}) - f'(\xi; \epsilon^*) = v'(\xi; \hat{\epsilon})(\epsilon^{**} - \epsilon^*) > M > 0$

It becomes contrary.

It is to mentioned that the bounds for skin friction factor are evaluated and presented in the next part. □

Bounds for skin friction factor. Bounds are derived for coefficient of skin friction $f''(1) = \epsilon^*$. As $f'(\xi;\epsilon^*)$ be a solution of the BVP to satisfy $f''(1;\epsilon^*) = \epsilon^* < 0$ and cannot have a maximum. It is claimed that for a solution to company the boundary condition (8), yields

$$f'''(1) = \frac{1}{(1+\frac{1}{\beta})}[Re - \epsilon(1+Re\gamma) + (M+K_p)] > 0 \tag{19}$$

Consider,

Case-1: Solutions with $f'(\xi;\epsilon^*) > 0$ for $\xi > 1$: let $f'''(1) < 0$ as f' is down concave initially. To satisfy Eq. (8), f' must change concavity at some point. For some ξ_3 such that $f'(\xi_3) > 0$, $f''(\xi_3) < 0$, and $f'''(\xi_3) = 0$ with $f^{iv}(\xi_3) \geq 0$. Differentiating Eq. (5), yields:

$$(1+\frac{1}{\beta})\xi f^{iv} + (2+\frac{1}{\beta}+Ref)f''' - Ref'f'' - (M+K_p)f'' = 0,\ 1 < \xi < \infty, \tag{20}$$

From Eq. (20), at $\xi = \xi_3$

$$(1+\frac{1}{\beta})\xi_3 f^{iv}(\xi_3) = Ref'(\xi_3)f''(\xi_3) + (M+K_p)f''(\xi_3) < 0 \tag{21}$$

Also, seen in Lemma 1, $f'''(\xi_3) = f''(\xi_3) = 0$, so it becomes contrary. Next let $f'''(1) = 0$, in Eq. (20) to get:

$$f^{iv}(1) = \frac{1}{(1+\frac{1}{\beta})}[Re + (M+K_p)]\epsilon < 0 \tag{22}$$

Then initially, $f''' < 0$ for $\xi > 1$, and f''' cannot change sign.

Case-2: Solution for which $f'(\xi;\epsilon^*) < 0$: let $f'''(1) < 0$ and f' is down concave initially. Because there exist a first point ξ_4 such that $f'(\xi_4) = 0$ and $f''(\xi_4) < 0$, f' is not positive for all ξ. Also, f' should be concave up to satisfy Eq. (8) for some $\xi > \xi_4$ and it attained a minimum. As f' does not attain maximum, f' necessarily increase from its minimum monotonically, and then tends to 0 from below to become concave down.

It becomes clear that, f''' must change sign from minus to plus and back to minus. Thus a point ξ_5 is such that f''' has a positive max, i.e., $f'''(\xi_5) > 0$, $f^{iv}(\xi_5) = 0$, and $f^{(v)}(\xi_5) \leq 0$. The Eq. (20) is differentiated and evaluated at ξ_5 to produce,

$$\xi_5 f^{(v)}(\xi_5) = \frac{1}{(1+\frac{1}{\beta})}Re(f''(\xi_5))^2 \geq 0 \tag{23}$$

If $f''(\xi_5) \neq 0$, contradiction is arrived: Taking the case $f''(\xi_5) = f^v(\xi_5) = 0$. The Eq. (20) is differentiated two times to have $f^{vi}(\xi_5) = 0$. Then Eq. (20) is differentiated thrice to get a result for $\xi = \xi_5$

$$\xi_5 f^{(vii)}(\xi_5) = \frac{1}{(1+\frac{1}{\beta})}2Re(f'''(\xi_5))^2 > 0.$$

So finally, $f^{iv}(\xi_5) = f^v(\xi_5) = f^{vi}(\xi_5) = 0$ with $f^{vii}(\xi_5) > 0$. For ξ nearly greater than ξ_5, f^{iv} is positive and f''' is increasing to contradict if f''' is to possess maximum at ξ_5. We have

$$f'''(1) = \frac{1}{(1+\frac{1}{\beta})}[Re - \epsilon^*(1+Re\gamma) + (M+K_p)] > 0 \tag{24}$$

This bounds provides useful information, if $\gamma \geq -\frac{1}{Re}$. However, we have

$$\frac{Re + (M+K_p)}{1+Re\gamma} < \epsilon^*,\ if\ \gamma < -\frac{1}{Re} \tag{25}$$

then an upper bound on ϵ^* can be attained if $\gamma \leq -\frac{2}{R}$. At this stage , it is assumed that

$$f^{iv}(1) = \frac{1}{(1+\frac{1}{\beta})}(Re+M+K_p)\epsilon - \frac{1}{(1+\frac{1}{\beta})}(2+\frac{1}{\beta}+Re\gamma)[Re-(1+Re\gamma)\epsilon + (M+K_p)] < 0 \tag{26}$$

First if $f^{iv}(1) > 0$, then there exists a first point ξ_6 such that $f^{vi}(\xi_6) = 0$ with $f^v(\xi_6) \leq 0$; otherwise,

$$f^{iv}(\xi) > 0,\ for\ \xi > 1 \tag{27}$$

It will leads to a contradiction. Integration of Eq. (27) yields:

$$f'''(\xi) > K,\ for\ \xi > 1 \tag{28}$$

where $K = \frac{1}{(1+\frac{1}{\beta})}[Re - \epsilon(1+Re\gamma) + (M+K_p)] > 0$. Integrating second time

$$f''(\xi) > \epsilon + K(\xi - 1),\ for\ \xi > 1 \tag{29}$$

When $\xi \to \infty$, let $f'' \to \infty$ then $f' \to 0$ as needed for Eq. (8).

γ	Lower bounds on $f''(1)$	$f''(1)$ num. approx	Upper bounds on $f''(1)$
− 0.5	NA	− 1.0007	NA
− 1.0	NA	− 0.8389	NA
− 3.0	− 0.600	− 0.4432	− 0.402
− 4.0	− 0.400	− 0.3414	− 0.340
− 6.0	− 0.240	− 0.2260	− 0.220
− 8.0	− 0.170	− 0.1663	− 0.160
− 10.0	− 0.133	− 0.1320	− 0.131

Table 1. Values of $f''(1)$ for $Re = 1, M = K_p = 0.1$ *and* $\beta = 10$.

Thus f^{iv} goes to decrease from 0 at some point ξ_6. Differentiate Eq. (20) and evaluate at ξ_6 to get

$$\xi_6 f^{(v)}(\xi_6) = Re(f''(\xi_6))^2 \geq 0$$

If $f''(\xi_6) \neq 0$, it makes a contradiction. If $f''(\xi_6) = 0$, then a similar procedure as above provides $f^{vi}(\xi_6) = 0$ and $f^{vii}(\xi_6) > 0$. Thus $f^{iv} > 0$ for right interval of ξ_6, it is not negative as needed, so $f^{iv}(1) \not> 0$.

If $f^{iv}(1) = 0$ then Eq. (24) becomes $f^{v}(1) = R\epsilon^2 > 0$ then contradiction is attained through above arguments. Solving for ϵ in Eq. (28) and using Eq. (25) yields.

$$\frac{Re + (M + K_p)}{1 + Re\gamma} < \epsilon^* < \frac{(Re + M + K_p)(2 + \frac{1}{\beta} + Re\gamma)}{(1 + \frac{1}{\beta})(R - M - K_p) + (2 + \frac{1}{\beta} + R\gamma)(1 + R\gamma)}, \text{ if } \gamma \leq -\frac{2}{R} \tag{30}$$

It can be noticed that both bounds converge to zero, and so, $f''(1)$ converges to zero as γ ($\gamma < 0$) tends to infinity. Computations of skin friction coefficient $f''(1) = \epsilon^*$ are provided in Table 1. Here sharpening of the bounds on $f''(1)$ is elucidated for a fixed a $Re = 1$, as the parameter γ enhances.

The bound are acceptable for the solutions of the BVP if $\gamma \leq -\frac{2}{R}$. Now we discuss the bounds for $\gamma > -\frac{1}{2R}$. firstly for $f'(\xi; \epsilon^*) > 0$ when $\xi > 1$, and secondly for $f'(\xi; \epsilon^* < 0)$. A lemma is presented for proof of Theorem 3.

Lemma 3 *Suppose* $f'(\xi; \epsilon^*) > 0$ *is solution of Eq.* (5) *with associated conditions* (8). *If* $\gamma > -\frac{1}{2Re}$, *then*

$$\lim_{\xi \to \infty} [-\xi(f''(\xi))^2 + \frac{2Re}{3}(f'(\xi))^3 + (M + K_p)(f'(\xi))^2] = 0.$$

Proof From theorem 1 we take $f'(\xi; \epsilon^*) > 0$ for $\xi > 1$ and $f''(\xi; \epsilon^*) < 0$ for $\xi > 1$. Then f is increasing and f' is decreasing function. As $\gamma > -\frac{1}{2Re}$, then $1 - \frac{1}{\beta} + 2Re\gamma > 0$ for $\xi > 1$. Multiplication of Eq. (5) with $f''(\xi)$ and integrating to get

$$\int_1^{\xi} (1 - \frac{1}{\beta} + 2Ref(z))(f''(z))^2 dz - (1 + \frac{1}{\beta})\epsilon^2 + \frac{2Re}{3} + (M + K_p) = (1 + \frac{1}{\beta})\xi(f''(\xi))^2 + \frac{2Re}{3}(f'(\xi))^3 + (M + K_p)(f'(\xi))^2 \Big\} \tag{31}$$

Here, the LHS of equation Eq. (31) is an increasing function and similarly the RHS. As $f'(\xi; \epsilon^*)$ is a solution to the B.V.P, we have $f' \to 0$ as $\xi \to \infty$. As $-(1 + \frac{1}{\beta})\xi(f''(\xi))^2$ increases and bounded above by 0, its limit as $\xi \to \infty$ exists.

Also let limit is $l \neq 0$. Since $\lim_{\xi \to \infty} f'(\xi) = 0$ and $-(1 + \frac{1}{\beta})\xi(f''(\xi))^2 < 0$ for $\xi > 1$, we must have $l < 0$. Suppose $l = -m$. Keeping in view That RHS of Eq. (31) is increasing, we have

$$-(1 + \frac{1}{\beta})\xi(f''(\xi))^2 + \frac{2R}{3}(f'(\xi))^3 + (M + K_p)(f'(\xi))^2 < -m \text{ for } \xi \geq 1$$

and by skipping second term on LHS to get:

$$(1 + \frac{1}{\beta})\xi(f''(\xi))^2 > m \text{ for } \xi \geq 1.$$

It implies as:

$$(f''(\xi) - \sqrt{\frac{m}{(1 + \frac{1}{\beta})\xi}})(f''(\xi) + \sqrt{\frac{m}{(1 + \frac{1}{\beta})\xi}}) > 0 \text{ for } \xi \geq 1,$$

As the second term on the left is negative,

$$f''(\xi) < \sqrt{\frac{m}{(1+\frac{1}{\beta})\xi}} \text{ for } \xi \geq 1.$$

Integration of this inequality provides as:

$$f'(\xi) < 1 - 2\sqrt{\frac{m}{(1+\frac{1}{\beta})}}(\sqrt{\xi} - 1) \text{ for } \xi \geq 1,$$

and let $\xi \to \infty$ then $f' \to -\infty$ which is contradiction to Eq. (8). □

Theorem 3 *Let $f'(\xi;\epsilon^*) > 0$ is a solution of Eq. (5)associated with boundary conditions (8).If $\gamma > -\frac{1}{2R}$, then $\epsilon^* < -\sqrt{\frac{1}{(1+\frac{1}{\beta})}[\frac{2Re}{3} + (M+K_p)]}$*

Proof Using Lemma 3 results and letting $\xi \to \infty$ in Eq. (31)

$$\int_1^{\xi} (1 - \frac{1}{\beta} + 2Ref(z))(f''(z))^2 dz = (1+\frac{1}{\beta})\epsilon^2 - \frac{2Re}{3} + (M+K_p) > 0,$$

since $1 - \frac{1}{\beta} + 2Rf > 0$ for $\xi > 1$. Thus $\epsilon^* < -\sqrt{\frac{1}{(1+\frac{1}{\beta})}[\frac{2Re}{3} + (M+K_p)]}$.

Although the existence of solutions where $f'(\xi;\epsilon^*) < 0$ is yet an open problem. Suppose such solution exist, then a bound on the skin friction coefficient is established in next Theorem 4. Two lemmas are required for the proof of this bounds.

Lemma 4 *suppose there exist a solution of Eq. (5) associated with boundary conditions (8) where $f'(\xi;\epsilon^*) < 0$. Then $\lim_{\xi\to\infty}(1+\frac{1}{\beta})\xi f''(\xi) = 0$.*

Proof In preview of the case $\gamma \leq -\frac{2}{Re}$, f' must attain a negative minimum and then turn concave down as $f' \to 0$ from below. Thus there exist a point ξ_7 such that $f' < 0$, $f'' > 0$, and $f''' < 0$ for $\xi > \xi_7$. By using these inequalities and rearranging Eq. (5) into the form

$$(1+\frac{1}{\beta})\xi f''' + (1+Ref)f'' - Re(f')^2 - (M+K_p)f' = 0,\ 1 < \xi < \infty, \tag{32}$$

It is concluded that $f(\xi) > -\frac{1}{Re}$ for $\xi > \xi_7$.

Hence f is decreasing and bounded below for $\xi > \xi_7$, and so, $f(\infty) = l \geq -\frac{1}{Re}$ where l is finite. This results in

$$\lim_{\xi\to\infty} Ref(\xi)f'(\xi) = 0. \tag{33}$$

Hence for all $\epsilon_1 > 0$, there is $\bar{\xi} > \xi_7$ to yield:

$$-\frac{\epsilon_1}{4} < Ref(\xi)f'(\xi) < \frac{\epsilon_1}{4} \text{ for } \xi > \bar{\xi}_7. \tag{34}$$

Keeping in view of contradiction, suppose that $\lim_{\xi\to\infty}(1+\frac{1}{\beta})\xi f''(\xi) \neq 0$, there exist an $\epsilon_1 > 0$ and a sequence $\xi_i \to \infty$ such that $|(1+\frac{1}{\beta})\xi_i f''(\xi_i)| \geq \epsilon_1$ for $i = 1, 2, ...$ and since $f'' > 0$ for $\xi > \bar{\xi}_7$, we have

$$(1+\frac{1}{\beta})\xi_i f''(\xi_i) \geq \epsilon_1 \text{ for } \xi_i > \xi_7. \tag{35}$$

For any positive integer N, the inequalities (34), (37) hold where $\xi_N > \bar{\xi} > \xi_7$. We get

$$(1+\frac{1}{\beta})\xi_i f''(\xi_i) + Ref(\xi_i)f'(\xi_i) > \epsilon_1 - \frac{\epsilon_1}{4} = \frac{3\epsilon_1}{4} \text{ for } \xi_i \geq \xi_N. \tag{36}$$

Arrangements of Eq. (13) yields

$$2Re\int_1^{\xi}(f'(z))^2 dz + Re\gamma + (1+\frac{1}{\beta})\epsilon = (1+\frac{1}{\beta})\xi f''(\xi) + Ref(\xi)f'(\xi) + Re[(M+K_p)(f(\xi)-\gamma)], \tag{37}$$

here LHS is increasing. It is concluded that the inequality (36) stands for all $\xi \geq \xi_N$ and (36) becomes

$$(1+\frac{1}{\beta})\xi f''(\xi) \geq \frac{3\epsilon_1}{4} - Ref(\xi)f'(\xi) \text{ for } \xi \geq \xi_N \tag{38}$$

and using (34) in (38) yields □$(1+\frac{1}{\beta})\xi f''(\xi) \geq \frac{\epsilon_1}{2}$ for $\xi \geq \xi_N$.

Dividing both sides by ξ and integrating results in $f'(\xi) \geq f'(\xi_N) + \frac{\epsilon_1}{2}[ln\xi - ln\xi_N]$ for $\xi \geq \xi_N$.
Finally, suppose $\xi \to \infty$ and $f' \to \infty$ which contradict Eq. (8) and thus proof of lemma is complete.

Lemma 5 *Let there exists a solution of Eq.* (5) *with boundary conditions* (8) *when* $f'(\xi;\epsilon^*) < 0$*provided that* $\gamma > -\frac{1}{2R}$, $\int_1^\infty (1 - \frac{1}{\beta} + 2Rf(z))(f''(z))^2 dz > 0$.

Proof It is sufficient to show that $1 - \frac{1}{\beta} + 2Rf > 0$ for $\xi \geq 1$. From Lemma 4,it is seen that $f' < 0$, $f'' > 0$ and $f''' < 0$ for $\xi > \xi_7$. Hence $f'' > 0$ and decreasing and $f'(\infty)$ exists, then $f''(\infty) = 0$. Suppose $\xi \to \infty$ in Eq. (31) and using Lemma 4 to get

$$\lim_{\xi\to\infty}[-\xi(f''(\xi))^2 + \frac{2Re}{3}(f'(\xi))^3 + (M + K_p)(f'(\xi))^2] = 0,$$

and thus

$$\int_1^\infty (1 - \frac{1}{\beta} + 2Ref(z))(f''(z))^2 dz = (1 + \frac{1}{\beta})\epsilon^2 - \frac{2Re}{3} + (M + K_p). \tag{39}$$

Also, we have

$$\left.\begin{aligned}\int_1^\xi (1 - \frac{1}{\beta} + 2Rf(z))(f''(z))^2 dz - (1 + \frac{1}{\beta})\epsilon^2 + \frac{2Re}{3} + (M + K_p) = \\ -(1 + \frac{1}{\beta})\xi(f''(\xi))^2 + (M + K_p)(f'(\xi))^2 + \frac{2R}{3}(f'(\xi))^3 < 0 \, for \, \xi > \xi_7\end{aligned}\right\} \tag{40}$$

It is to note that both terms on the right are negative, and so,

$$\int_1^\xi (1 - \frac{1}{\beta} + 2Ref(z))(f''(z))^2 dz = (1 + \frac{1}{\beta})\epsilon^2 - \frac{2Re}{3} + +(M + K_p) \, for \, \xi > \xi_7. \tag{41}$$

Thus $\int_1^\xi (1 - \frac{1}{\beta} + 2Ref(z))(f''(z))^2 dt$ tends to infinity from below, and $1 - \frac{1}{\beta} + 2Ref$ is to be positive for large values of ξ. Since $\gamma > -\frac{1}{2Re}$, and $1 - \frac{1}{\beta} + 2Ref$ starts out positive because f' has only one sign change – from positive to negative $-f$ attains one maximum and so does $1 - \frac{1}{\beta} + 2Ref$. Thus $1 - \frac{1}{\beta} + 2Ref > 0$ for $\xi \geq 1$ and hence, the proof of lemma.

Theorem 4 *Let there is a solution for Eq.* (5) *associated with the boundary conditions* (8) *where* $f'(\xi;\epsilon^*) < 0$. *If* $\gamma > -\frac{1}{2Re}$, *then* $\epsilon^* < min[-\sqrt{\frac{1}{(1+\frac{1}{\beta})}[\frac{2Re}{3} + (M + K_p)]}, -\frac{Re\gamma}{(1+\frac{1}{\beta})}]$.

Proof Suppose $\xi \to \infty$, using Lemma 4, Eq. (33) in Eq. (37) to achieve as below

$$\left.\begin{aligned}\int_1^\infty (f''(z))^2 dz = \left(\frac{\left(1 + \frac{1}{\beta}\right)\epsilon + Re\gamma}{2Re}\right) > 0, \\ \epsilon^* < -\frac{Re\gamma}{\left(1 + \frac{1}{\beta}\right)}\end{aligned}\right\} \tag{42}$$

Using Lemma 5 in Eq. (41) to get

$$\epsilon^* < -\sqrt{\frac{1}{(1 + \frac{1}{\beta})}[\frac{2Re}{3} + (M + K_p)]}, \; if \; \gamma > -\frac{1}{2Re}, \tag{43}$$

From combining the inequalities (42), (43), we get $\epsilon^* < min[-\sqrt{\frac{1}{(1+\frac{1}{\beta})}[\frac{2Re}{3} + (M + K_p)]}, -\frac{Re\gamma}{(1+\frac{1}{\beta})}]$, if $\gamma > -\frac{1}{2Re}$.

□

Results and discussion

The current results are checked for validation as listed in Table 2 and 3. Their acceptable accord with those by Mastroberardino and Siddique[41] has established the accuracy of the present numeric scheme. The pictorial representation for Casson nano-fluid's velocity, temperature and concentration of nano-entities graphed for two cases of mass transpiration ($\gamma > 0, \gamma < 0$).

The outcomes for velocity $f'(\xi)$, temperature $\theta'(\xi)$ and concentration $\phi'(\xi)$ are sketched in Figs. 2, 3, 4 and 5 for two cases of γ ($\gamma = -0.5 and \gamma = 0.5$) with the variation of other influential parameters. The velocity $f'(\xi)$ is vividly decelerated against the increments in magnetic parameter M as well as that of porosity parameter K_p as seen in Fig. 2. The strength of M means growth of electromagnetic resistive force (Lorentz force) which inhibits the flow. Similarly, parameter of porous matrix (K_p) offers enhanced resistance to the velocity. There is sound

M	Re	$\gamma = 0.5$[41]	$\gamma = 0.5$ (Present results)	Percentage deviation	$\gamma = -0.5$[41]	$\gamma = -0.5$ (present results)	Percentage deviation
0	10	− 6.62227	− 6.6223	0.000453	− 1.67757	− 1.6778	− 0.013710
2		− 6.88470	− 6.8847	0.000000	− 1.92938	− 1.9294	0.001036
5	10	− 7.24505	− 7.2451	0.000690	− 2.27933	− 2.2793	− 0.001316
2	1	− 2.21659	− 2.2180	0.063611	− 1.72075	− 1.7214	0.037774
	5	− 4.33228	− 4.3330	0.016619	− 1.86364	− 1.8638	0.008585
	10	− 6.88470	− 6.8847	0.000000	− 1.92938	− 1.9294	0.001036

Table 2. The skin friction coefficient by varying M and Re.

γ	Re	M	Pr	Mastroberardino and Siddique[41]	Present results	Percentage deviation
0.5	10	2	7	36.60283	36.6027	− 0.0003551
0.0				6.08375	6.0857	0.0320525
− 0.5				0.00002	0.00002	0.0000000
0.5	1			4.57611	4.5741	− 0.0439237
	5			18.99556	18.9952	− 0.0018951
	10			36.60283	36.6027	− 0.0003551
	10	0		36.60105	36.6115	0.0285510
		2		36.60283	36.6027	− 0.0003551
		5		36.60551	36.5906	− 0.0407315
		2	0.7	4.18133	4.1801	− 0.294164
			2	11.13801	11.1360	− 0.0180463
			7	36.60283	36.6027	− 0.0003551

Table 3. Nusselt number table for varying γ, Re, M, and Pr.

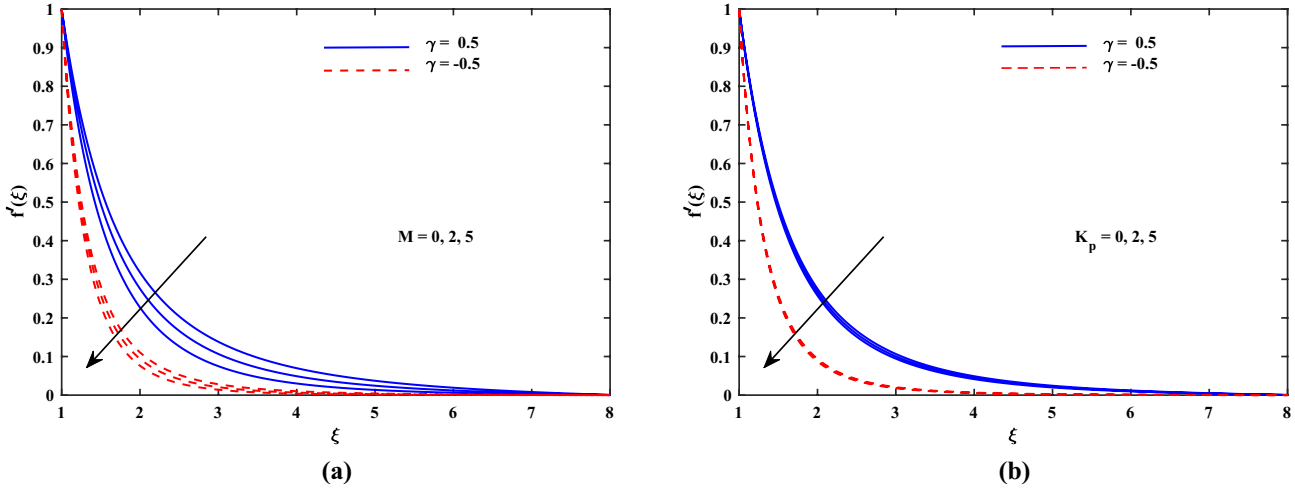

Figure 2. Plot for velocity profile $f'(\xi)$ with varying values of M and K_p.

reason behind this fact that K_p is related reciprocally with permeability and hence higher inputs of K_p means lesser permeability. Thus the flow decelerates in this case. The incremented values of Re and Casson parameter β also slowed the flow velocity $f'(\xi)$ as delineated in Fig. 3. Here the viscous effects are enhanced (to oppose to) momentum. Furthermore, it is noticed that velocity of flow is faster in case of injection ($\gamma > 0$) than for suction ($\gamma < 0$). Figure 4 exposed that the nanofluid diffusion parameters namely Nb (Brownian diffusion) and Nt (Thermophoresis diffusion) are responsible to raise the temperature function $\theta(\xi)$ but the progressive values of Pr reduced $\theta(\xi)$. The faster random motion of nano-entities is associated with larger Nb. This rapidity in the movement of these small material particles causes greater thermal distribution. In the similar behavior due to enhanced enhanced thermophoresis. The particles move fastly towards cooler regimes and hence raises the temperature. It is also noticed that the fluid temperature for suction is higher than for injection. The greater values of Le and Re diminish the nanoparticle concentration $\phi(\xi)$ in the boundary layer region as depicted in Fig. 5. Physically, the

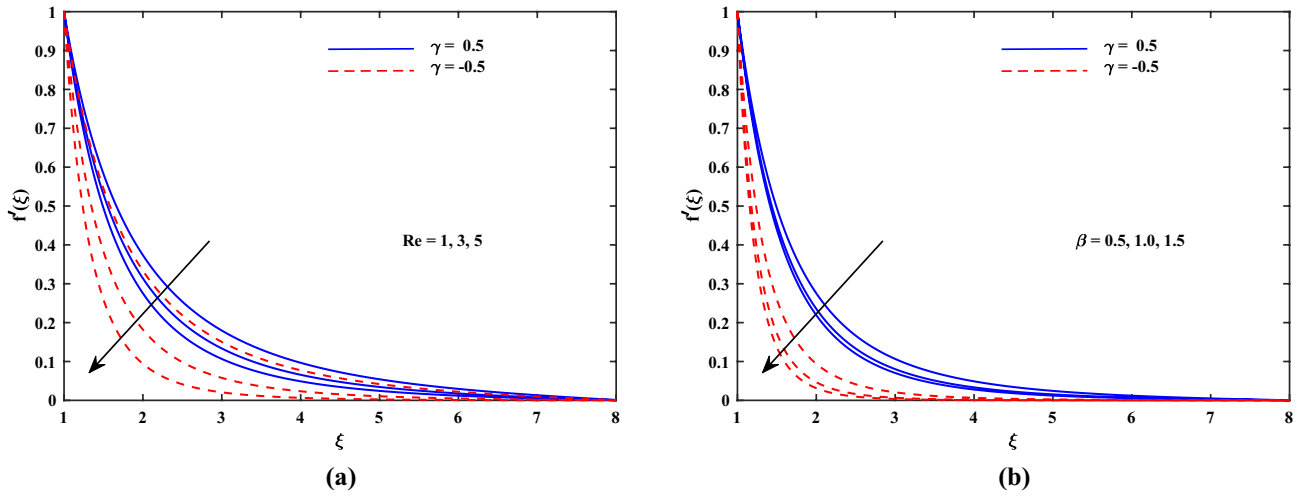

Figure 3. Plot for velocity profile $f'(\xi)$ with varying values of Re and β.

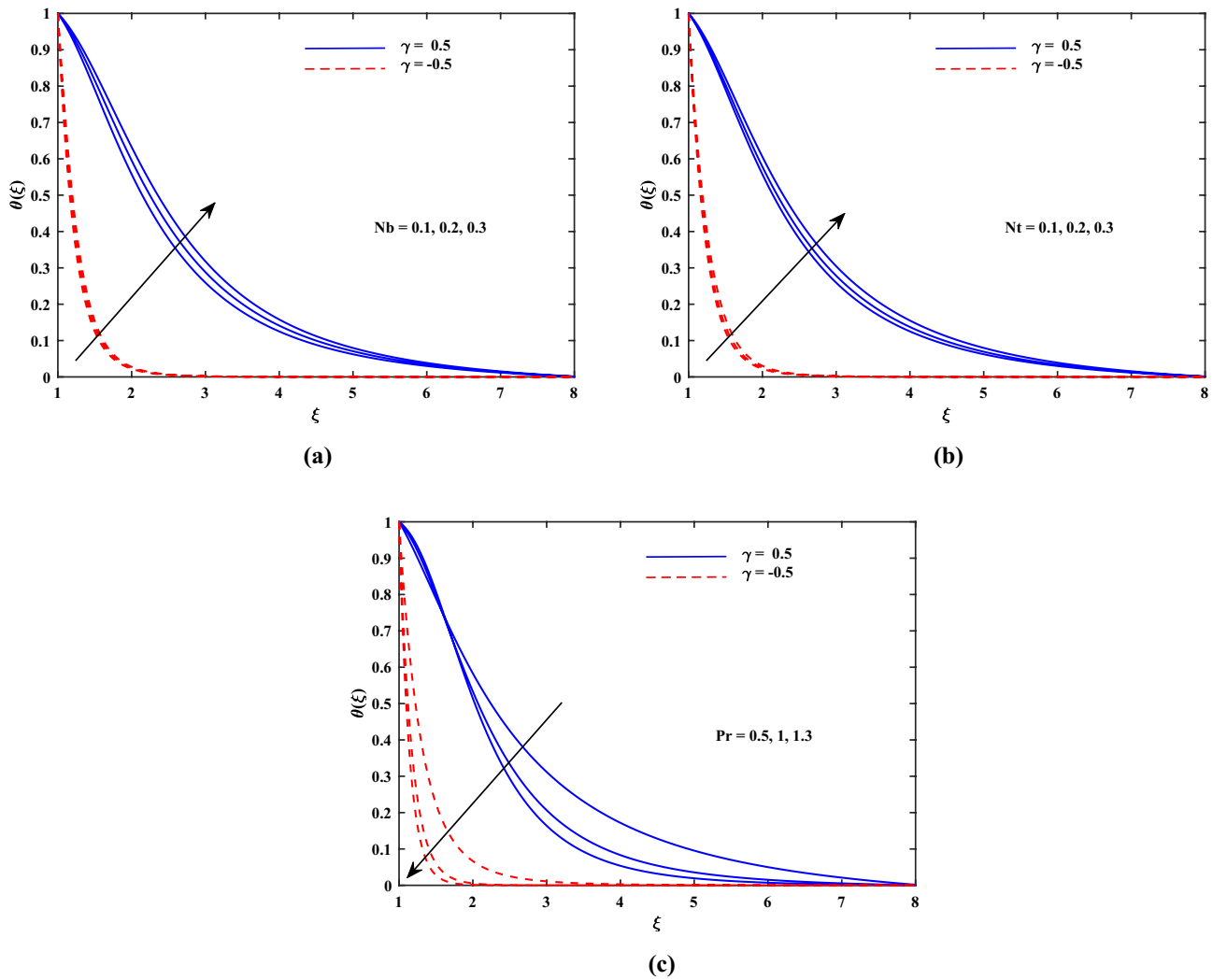

Figure 4. Plot for temperature profile $\theta(\xi)$ with varying values of Nb, Nt and Pr.

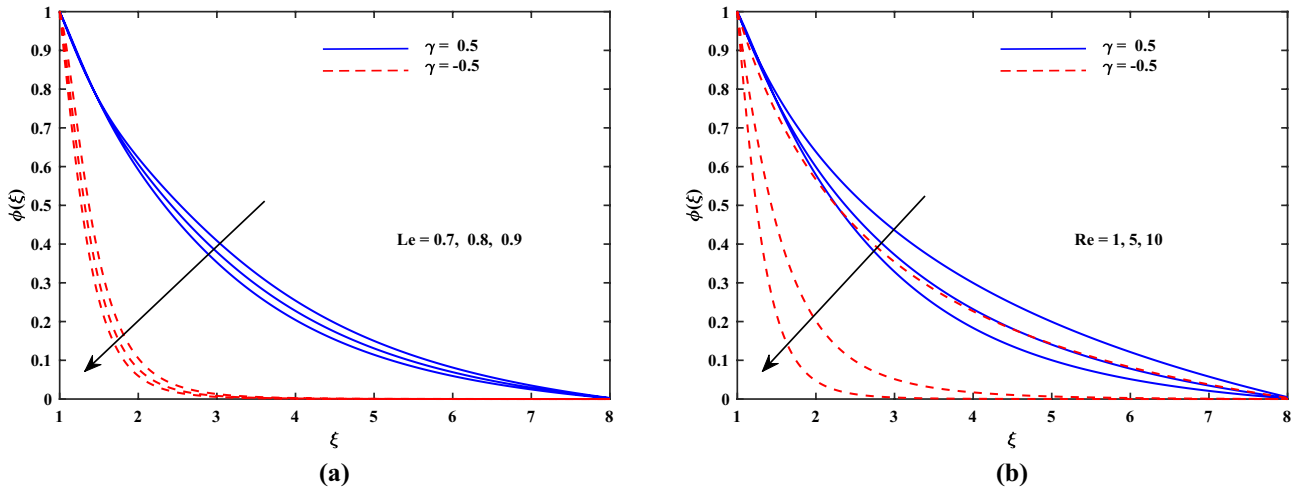

Figure 5. Plot for concentration profile $\phi(\xi)$ with varying values of *Le* and *Re*.

K_p	M	Re	β	$\gamma = -0.5$	$\gamma = 0$	$\gamma = 0.5$
0.5	2	10	0.5	1.5608	2.2392	3.1970
1.0				1.6001	2.2818	3.2380
1.5				1.6386	2.3234	3.2781
0.5	0			1.3953	2.0576	3.0218
	2			1.5608	2.2392	3.1970
	5			1.7862	2.4814	3.4307
	2	1		1.2200	1.3002	1.3851
		5		1.4208	1.7861	2.2385
		10		1.5608	2.2392	3.1970
		10	0.5	1.5608	2.2392	3.1970
			1.0	1.7271	2.6988	4.1909
			1.5	1.8000	2.9378	4.7615

Table 4. Skin friction $-f''(0)$ for varying K_p, M, Re, and β.

Pr	Nb	Nt	Le	Re	$-\theta'(0)$	$-\phi'(0)$
0.72	0.1	0.1	1	10	4.2980	
0.1					5.6546	
1.3					7.0521	
0.72	0.1				4.2980	
	0.2				4.1206	
	0.3				3.9488	
	0.1	0.1			4.2980	
		0.2			4.2028	
		0.3			4.1100	
		0.1	1			2.4484
			2			7.8881
			3			13.1081
			1	1		0.6743
				5		1.4877
				10		2.4484

Table 5. Nusselt number $-\theta'(0)$ and Sharwood number $-\phi'(0)$ for varying Pr, Nb, Nt, Le and Re .

Lewis number *Le* is inversely related to diffusion coefficient of concentration and hence its development impairs $\phi(\xi)$. Moreover as seen above, the larger *Re* slows the flow which results in decrement of $\phi(\xi)$

The absolute values of skin friction are augmented in direct proportion with K_p, *M*, *Re* and β for three cases of γ ($\gamma < 0, \gamma = 0, \gamma > 0$) as enumerated in Table 4. Physically, K_p signifies the resistance of porous matrix, *M* for electromagnetic resistive force, *Re* (Reynolds number) and β the non-Newtonian viscous effects (for Casson fluid). Hence the drag force enhances. Table 5 indicates that Nusselt number $-\theta'(0)$ increases with *Pr* but it diminishes against *Nb* and *Nt*. Physical ground for augmentation of Nusselt number with Prandtl number lies in the fact that thermal diffusivity being reciprocal to prandtl number is responsible to decrease the temperature of the fluid and more heat transfer takes place at the surface and hence the magnitude of Nusselt number is boosted. Further the growing thermopherotic and Brownian diffusion raise the fluid temperature and heat transfer rate at the surface is decreased and the Nusselt number decreases against these parameters. Also, the Sherwood number $-\phi'(0)$ exceeds directly with *Le* and *Re* (see Table 5).

Conclusion

We discussed the existence of solution for Casson fluid flow towards a porous stretching cylinder. The fluid flows through porous medium and it is influenced by magnetic field. It is shown that the boundary value problem for any $Re > 0$ and $-\infty < \gamma < \infty$, to satisfy $f'(\xi) > 0$ and $f''(\xi) < 0$ for all $\xi > 1$. The uniqueness of the result is established in the sense that we cannot have two solutions for the boundary value problem if $-\infty < \gamma < \infty$ and $Re > 0$. Moreover, the bounds for skin friction factor are evaluated. Numerical solution of the flow and heat transfer for Casson nano-fluid is also obtain to reveal that:

- It is observed that for the magnetic parameter *M* and porosity parameter *kp* reduces velocity when takes large values for three cases of γ.
- Velocity recedes with the higher inputs of *Re* and β.
- Temperature decreases with the boosting values of *Pr* but it uplifted with higher values of *Nb* and *Nt*.
- *Le* and *Re* cause deprecation in concentration when takes larger values.
- Skin friction factor is boosted up significantly when takes larger K_p, *M*, *Re* and β.
- Nusselt number and Sherwood number up surged directly with larger *Pr*, *Le* and *Re* while recedes for larger *Nb* and *Nt*.

Received: 5 January 2021; Accepted: 22 March 2021
Published online: 08 April 2021

References

1. Shah, Z., Kumam, P. & Deebani, W. Radiative MHD Casson nanofluid flow with activation energy and chemical reaction over past nonlinearly stretching surface through entropy generation. *Sci. Rep.* **10**, 1–14 (2020).
2. Oyelakin, I., Mondal, S., Sibanda, P. & Sibanda, D. Bioconvection in Casson nanofluid flow with gyrotactic microorganisms and variable surface heat flux. *Int. J. Biomath.* **12**, 1950041 (2019).
3. Reza-E-Rabbi, S., Arifuzzaman, S., Sarkar, T., Khan, M. S. & Ahmmed, S. F. Explicit finite difference analysis of an unsteady MHD flow of a chemically reacting Casson fluid past a stretching sheet with brownian motion and thermophoresis effects. *J. King Saud Univ. Sci.* **32**, 690–701 (2020).
4. Oyelakin, I. S., Mondal, S. & Sibanda, P. Unsteady Casson nanofluid flow over a stretching sheet with thermal radiation, convective and slip boundary conditions. *Alexandria Eng. J.* **55**, 1025–1035 (2016).
5. Oyelakin, I., Lalramneihmawii, P., Mondal, S. & Sibanda, P. Analysis of double-diffusion convection on three-dimensional mhd stagnation point flow of a tangent hyperbolic casson nanofluid. *Int. J. Ambient Energy* **1–12**, (2020).
6. Mondal, S., Oyelakin, I. & Sibanda, P. Unsteady mhd three-dimensional casson nanofluid flow over a porous linear stretching sheet with slip condition. *Front. Heat Mass Transfer* **8**, (2017).
7. Ali, L., Liu, X., Ali, B., Mujeed, S. & Abdal, S. Finite element simulation of multi-slip effects on unsteady MHD bioconvective micropolar nanofluid flow over a sheet with solutal and thermal convective boundary conditions. *Coatings* **9**, 842 (2019).
8. Ali, B., Nie, Y., Khan, S. A., Sadiq, M. T. & Tariq, M. Finite element simulation of multiple slip effects on MHD unsteady Maxwell nanofluid flow over a permeable stretching sheet with radiation and thermo-diffusion in the presence of chemical reaction. *Processes* **7**, 628 (2019).
9. Abdal, S., Ali, B., Younas, S., Ali, L. & Mariam, A. Thermo-diffusion and multislip effects on MHD mixed convection unsteady flow of micropolar nanofluid over a shrinking/stretching sheet with radiation in the presence of heat source. *Symmetry* **12**, 49 (2020).
10. Ali, L., Liu, X., Ali, B., Mujeed, S. & Abdal, S. Finite element analysis of thermo-diffusion and multi-slip effects on MHD unsteady flow of casson nano-fluid over a shrinking/stretching sheet with radiation and heat source. *Appl. Sci.* **9**, 5217 (2019).
11. Yu, B., Chiu, H.-T., Ding, Z. & Lee, L. J. Analysis of flow and heat transfer in liquid composite molding. *Int. Polym. Process.* **15**, 273–283 (2000).
12. Sakiadis, B. C. Boundary-layer behavior on continuous solid surfaces: I. boundary-layer equations for two-dimensional and axisymmetric flow. *AIChE J.* **7**, 26–28 (1961).
13. Sakiadis, B. Boundary-layer behavior on continuous solid surfaces: Ii. the boundary layer on a continuous flat surface. *AiChE J.* **7**, 221–225 (1961).
14. Awaludin, I. S., Ishak, A. & Pop, I. On the stability of MHD boundary layer flow over a stretching/shrinking wedge. *Sci. Rep.* **8**, 1–8 (2018).
15. Dzulkifli, N. F., Bachok, N., Yacob, N. A., Md Arifin, N. & Rosali, H. Unsteady stagnation-point flow and heat transfer over a permeable exponential stretching/shrinking sheet in nanofluid with slip velocity effect: A stability analysis. *Appl. Sci.* **8**, 2172 (2018).
16. Bakar, N. A. A., Bachok, N., Arifin, N. M. & Pop, I. Stability analysis on the flow and heat transfer of nanofluid past a stretching/shrinking cylinder with suction effect. *Results Phys.* **9**, 1335–1344 (2018).

17. Malvandi, A., Hedayati, F. & Ganji, D. Nanofluid flow on the stagnation point of a permeable non-linearly stretching/shrinking sheet. *Alexandria Eng. J.* **57**, 2199–2208 (2018).
18. Hayat, T., Riaz, R., Aziz, A. & Alsaedi, A. Influence of arrhenius activation energy in mhd flow of third grade nanofluid over a nonlinear stretching surface with convective heat and mass conditions. *Physica A* **124006** (2020).
19. Dinh, M. T. *et al.* Nanomaterial treatment due to imposing MHD flow considering melting surface heat transfer. *Physica A* **541**, 123036 (2020).
20. Rashid, I., Sagheer, M. & Hussain, S. Entropy formation analysis of MHD boundary layer flow of nanofluid over a porous shrinking wall. *Physica A* **536**, 122608 (2019).
21. Pavar, P., Krishna, L. H. & Reddy, M. S. Mhd flow of nano fluid past a vertical permeable semi-infinite moving plate with constant heat source. In *AIP Conference Proceedings*, vol. 2246, 020020 (AIP Publishing LLC, 2020).
22. Oyelakin, I. S., Lalramneihmawii, P., Mondal, S., Nandy, S. K. & Sibanda, P. Thermophysical analysis of three-dimensional magnetohydrodynamic flow of a tangent hyperbolic nanofluid. *Eng. Rep.* **2**, e12144 (2020).
23. Chen, B.-S. *et al.* Entropy generation in mixed convection magnetohydrodynamic nanofluid flow in vertical channel. *Int. J. Heat Mass Transfer* **91**, 1026–1033 (2015).
24. Arifuzzaman, S. *et al.* Hydrodynamic stability and heat and mass transfer flow analysis of MHD radiative fourth-grade fluid through porous plate with chemical reaction. *J. King Saud Univ. Science* **31**, 1388–1398 (2019).
25. Khan, M. S., Zou, R. & Yu, A. Computational simulation of air-side heat transfer and pressure drop performance in staggered mannered twisted oval tube bundle operating in crossflow. *Int. J. Thermal Sci.* **161**, 106748 (2021).
26. Choi, S. U. & Eastman, J. A. Enhancing thermal conductivity of fluids with nanoparticles. Tech. Rep.,Argonne National Lab., IL (United States) (1995).
27. Mahdavi, M., Sharifpur, M. & Meyer, J. P. Fluid flow and heat transfer analysis of nanofluid jet cooling on a hot surface with various roughness. *Int. Commun. Heat Mass Transfer* **118**, 104842 (2020).
28. Oyelakin, I., Mondal, S. & Sibanda, P. Nonlinear radiation in bioconvective Casson nanofluid flow. *Int. J. Appl. Comput. Math.* **5**, 1–20 (2019).
29. Ali, B., Naqvi, R. A., Ali, L., Abdal, S. & Hussain, S. A comparative description on time-dependent rotating magnetic transport of a water base liquid h2o with hybrid nano-materials al2o3-cu and al2o3-tio2 over an extending sheet using buongiorno model: Finite element approach. *Chin. J. Phys.* (2021).
30. Ali, B., Hussain, S., Abdal, S. & Mehdi, M. M. Impact of Stefan blowing on thermal radiation and Cattaneo–Christov characteristics for nanofluid flow containing microorganisms with ablation/accretion of leading edge: Fem approach. *Eur. Phys. J. Plus* **135**, 1–18 (2020).
31. Naga Santoshi, P., Ramana Reddy, G. & Padma, P. Numerical scrutinization of three dimensional Casson–Carreau nano fluid flow. *J. Appl. Comput. Mech.* **6**, 531–542 (2020).
32. Reza-E-Rabbi, S., Ahmmed, S. F., Arifuzzaman, S., Sarkar, T. & Khan, M. S. Computational modelling of multiphase fluid flow behaviour over a stretching sheet in the presence of nanoparticles. *Eng. Sci. Technol.* **23**, 605–617 (2020).
33. Sadeghi, M., Tayebi, T., Dogonchi, A., Nayak, M. & Waqas, M. Analysis of thermal behavior of magnetic buoyancy-driven flow in ferrofluid-filled wavy enclosure furnished with two circular cylinders. *Int. Commun. Heat Mass Transfer* **104951** (2020).
34. Seyyedi, S. M., Dogonchi, A., Nuraei, R., Ganji, D. & Hashemi-Tilehnoee, M. Numerical analysis of entropy generation of a nanofluid in a semi-annulus porous enclosure with different nanoparticle shapes in the presence of a magnetic field. *Eur. Phys. J. Plus* **134**, 1–20 (2019).
35. Dogonchi, A. *et al.* The influence of different shapes of nanoparticle on cu-h2o nanofluids in a partially heated irregular wavy enclosure. *Physica A* **540**, 123034 (2020).
36. Seyyedi, S. M., Dogonchi, A., Hashemi-Tilehnoee, M., Waqas, M. & Ganji, D. Investigation of entropy generation in a square inclined cavity using control volume finite element method with aided quadratic lagrange interpolation functions. *Int. Commun. Heat Mass Transfer* **110**, 104398 (2020).
37. Dogonchi, A., Waqas, M., Seyyedi, S. M., Hashemi-Tilehnoee, M. & Ganji, D. A modified Fourier approach for analysis of nanofluid heat generation within a semi-circular enclosure subjected to mfd viscosity. *Int. Commun. Heat Mass Transfer* **111**, 104430 (2020).
38. Dogonchi, A., Asghar, Z. & Waqas, M. Cvfem simulation for fe3o4-h2o nanofluid in an annulus between two triangular enclosures subjected to magnetic field and thermal radiation. *Int. Commun. Heat Mass Transfer* **112**, 104449 (2020).
39. Sadeghi, M. S., Tayebi, T., Dogonchi, A. S., Armaghani, T. & Talebizadehsardari, P. Analysis of hydrothermal characteristics of magnetic Al2O3-H2O nanofluid within a novel wavy enclosure during natural convection process considering internal heat generation. *Math. Methods Appl. Sci.* (2020).
40. Seyyedi, S. M., Dogonchi, A., Hashemi-Tilehnoee, M., Waqas, M. & Ganji, D. Entropy generation and economic analyses in a nanofluid filled l-shaped enclosure subjected to an oriented magnetic field. *Appl. Therm. Eng.* **168**, 114789 (2020).
41. Mastroberardino, A. & Siddique, J. Magnetohydrodynamic stagnation flow and heat transfer towards a stretching permeable cylinder. *Adv. Mech. Eng.* **6**, 1–5 (2014).
42. Sarojamma, G. & Vendabai, K. Boundary layer flow of a Casson nanofluid past a vertical exponentially stretching cylinder in the presence of a transverse magnetic field with internal heat generation/absorption. *Int. J. Math. Comput. Sci.* **9**, 138–143 (2015).

Author contributions

S.A.: Conceptualization, methodology, design; S.H.: Data curation, writing—original draft preparation. A.A. and I.S.: Supervision and validation of data—reviewing original draft. M.F.: Supervision, Reviewing and editing the final version and validation of data.

Competing interests

The authors declare no competing interests.

Additional information

Correspondence and requests for materials should be addressed to A.A.

Reprints and permissions information is available at www.nature.com/reprints.

Publisher's note Springer Nature remains neutral with regard to jurisdictional claims in published maps and institutional affiliations.